

# Influence of the R $\rightarrow$ T Transition on the Optical Absorption and Magnetic Circular Dichroism Spectra of Methemoglobin Fluoride, Aquomethemoglobin, and Hydroxymethemoglobin<sup>†</sup>

Marianne J. F. Rots and Pieter J. Zandstra\*

**ABSTRACT:** From the observed absorption spectra of methemoglobin fluoride (metHbF) and hemoglobin monoxide (HbCO) and the magnetic circular dichroism (MCD) spectrum of HbCO, molecular quantities of the high-spin ferric heme group of metHbF and the MCD spectra of metHbF can be calculated [Rots, M. J. F., & Zandstra, P. J. (1982) *Mol. Phys.* 46, 1283]. In an essentially similar procedure and with the molecular quantities obtained for metHbF (in the quaternary R state), the contributions of the high-spin fractions to the absorption and MCD spectra of metHbF in the quaternary T structure and of aquo- and hydroxymethemoglobin (metHbH<sub>2</sub>O and metHbOH, respectively) in both the R and the T states are estimated. In these calculations, the energy of the iron  $e_g^d$  orbital, which participates in the charge-transfer (CT) transitions, is used as an adjustable parameter. The changes in the absorption and MCD spectra of metHbF and metHbH<sub>2</sub>O upon the R  $\rightarrow$  T transition are supposed to arise solely from the changes in the contributions of the high-spin

fractions to the spectra, due to the change in energy of the iron  $e_g^d$  orbital. The calculation shows that a decrease in the energy of the iron  $e_g^d$  orbital of 0.017 and 0.008 eV for metHbF and metHbH<sub>2</sub>O, respectively, is likely, upon the R  $\rightarrow$  T transition. The lowering of the  $e_g^d$  orbital of the high-spin form of metHbOH is arbitrarily chosen as the average of these values. In the calculations for metHbOH, the increase of the high-spin fraction upon the R  $\rightarrow$  T transition is taken into account. With the spectra obtained for metHbH<sub>2</sub>O and metHbOH in the R and T states, difference spectra are calculated for methemoglobin at a series of pH values at which metHbH<sub>2</sub>O and metHbOH (metHbH<sub>2</sub>O/OH) occur simultaneously. The calculated spectra compared reasonably well with the experimental ones. Our results support the view held by Perutz et al. [Perutz, M. F., Heidner, E. J., Ladner, J. E., Beeststone, J. G., Ho, C., & Slade, E. F. (1974) *Biochemistry* 13, 2187] that the R  $\rightarrow$  T transition reduces the energy of the transitions from the porphyrin  $\pi$  to the iron  $e_g^d$  orbitals.

In previous publications (Rots & Zandstra, 1982; Rots, 1982), the absorption and magnetic circular dichroism (MCD) spectra of high-spin methemoglobin fluoride (metHbF) were described in the 350–1000-nm region with a molecular orbital model. In this model, which is referred to as the heme-F model, it is assumed that in zeroth order, four charge-transfer (CT) transitions of the type  $\pi \rightarrow d$  and two  $\pi \rightarrow \pi^*$  transitions are present. Various molecular quantities, such as the energy of the  $\pi \rightarrow d$  CT transitions, are determined in a semiempirical way by using inter alia a computer fit of the absorption spectrum of metHbF. Subsequently, the data thus obtained are used to calculate the (temperature-dependent) MCD spectra of metHbF.

We now present absorption and MCD spectra calculated for other high-spin ferric heme groups. These spectra are obtained by repeating the latter part of the calculation for metHbF with the molecular quantities obtained for metHbF and one adjustable parameter. In this way, spectra are calculated for metHbF in the quaternary T state and for the high-spin ferric heme groups that occur in aquomethemoglobin (metHbH<sub>2</sub>O) and hydroxymethemoglobin (metHbOH) in both the R and the T structures.

The R  $\rightarrow$  T structural changes are brought about by the addition of inositol hexaphosphate (IHP) (Fermie & Perutz, 1977; Perutz et al., 1974; Perutz, 1979). Perutz has given criteria to determine whether the quaternary structure is predominantly R or T, such as the differences in absorption and circular dichroism (CD) in the near-ultraviolet region

260–300 nm. Comparisons with spectral changes on R  $\rightarrow$  T transitions, without the use of IHP, establish that the change of the quaternary structure is mainly responsible for the observed spectral behavior (Perutz et al., 1974a,b, 1978, 1979).

Perutz et al. (1974) tentatively assigned the spectral changes observed for the R  $\rightarrow$  T transition in metHbF to a lowering of the CT energies, due to an increase of the Fe–N bond lengths. Asher et al. (1981), however, concluded from their resonance Raman spectra that the change in quaternary structure in metHbF causes mainly changes in the porphyrin part of the heme while no significant changes at or near the iron are supposed to occur.

In this work, it is investigated whether the changes of the absorption and MCD spectra of metHbF and metHbH<sub>2</sub>O may be accounted for by assuming that the only significant change upon the R  $\rightarrow$  T transition occurs at the iron. This was done by using the energy of the iron  $e_g^d$  orbital as the only adjustable parameter in the calculation of the high-spin ferric heme spectra. The spectra of the high-spin fractions of metHbOH in the R and T states were calculated similarly. Thus, the high-spin spectra of all six cases studied only differ in the calculations of the energy of the  $e_g^d$  orbital.

Calculations are also presented for the spectra of the mixtures of metHbH<sub>2</sub>O and metHbOH (metHbH<sub>2</sub>O/OH) at different pH. In the case of metHbOH, the R  $\rightarrow$  T transition, induced by IHP, shifts the equilibrium to the high-spin side (Perutz et al., 1978; Linder et al., 1980; Messana et al., 1978). The spectral simulations were done by using known equilibrium data and the same data for the high-spin spectra as mentioned above. The similarity between experimental and simulated spectra is rather satisfactory.

It may be mentioned that in the past some confusion about the changes of the absorption spectra on the R  $\rightarrow$  T transition in such mixtures has arisen because of the neglect of changes

<sup>†</sup> From the Department of Physical Chemistry, University of Groningen, Nijenborgh 16, 9747 AG Groningen, The Netherlands. Received April 15, 1983. The present investigation has been supported by the Netherlands Foundation for Chemical Research (SON) with financial aid from the Netherlands Organization for the Advancement of Pure Research (ZWO).

Table I: Conditions Used for Measurements of Spectra of metHbF and metHbH<sub>2</sub>O/OH in R and T State

derivative	pH	buffer <sup>a</sup>	[IHP]/[Hb tetramer]
metHbF	6.50	0.05 M Bis-Tris + 0.1 M KF	2
metHbH <sub>2</sub> O	5.80	0.05 M Bis-Tris + 0.1 M NaCl	3
metHbH <sub>2</sub> O/ OH	6.20	0.05 M Bis-Tris + 0.1 M NaCl	2
	6.83	0.05 M Bis-Tris + 0.1 M NaCl	2
	7.18	0.05 M Tris + 0.1 M NaCl	4
	7.45	0.05 M Tris + 0.1 M NaCl	8
metHbOH	10.2	0.10 M borate-NaOH	

<sup>a</sup> Bis-Tris, 2-[bis(2-hydroxymethyl)amino]-2-(hydroxymethyl)-1,3-propanediol; Tris, tris(hydroxymethyl)aminomethane.

of the spectrum of the high-spin form itself due to this transition. Also, following Smith & Williams (1970), spectral bands of the high-spin form have been ascribed to the low-spin form (Perutz et al., 1978; Linder et al., 1980), i.e., the 540–570-nm bands in metHbF (Rots & Zandstra, 1982).

### Materials and Methods

Absorption and MCD spectra were measured and metHbF samples were prepared as described by Rots & Zandstra (1982). metHbH<sub>2</sub>O/OH samples were prepared similarly, but in buffers containing NaCl instead of KF. The buffers used are listed in Table I.

In order to obtain metHb samples in the R and T states with the same concentration, a metHb sample was split into two parts of equal weight. To one part was added an appropriate amount of IHP, diluted with buffer and adjusted to the pH of the sample. Since the addition of IHP raises the pH of the sample (Perutz et al., 1974), it was titrated back to the desired pH, with the same buffer but of lower pH. The other sample was diluted with a corresponding amount of buffer. The concentration of IHP relative to the Hb concentration that was used is given in Table I. At pH > 7, higher concentrations of IHP were chosen to compensate for the reduced binding constant (Perutz et al., 1974b). Absorption and CD spectra in the 260–300-nm region were used to check the difference in quaternary structure between the two samples (Perutz et al., 1974). The Hb concentrations were determined by converting the samples to metHbCN. The absorption spectra of metHbCN in the visible region are the same in the absence and presence of IHP (Perutz et al., 1974). The concentrations used were 0.2–1.2 mM heme for measurements in the visible and infrared regions and 0.04–0.11 mM heme for the Soret region. The samples were measured in quartz cells, the thickness being chosen to give an optical density between 0.5 and 1.5. All absorption spectra are measured at room temperature. The MCD spectra are measured at 7 °C.

### Theory

We give a brief summary of the procedure used for the calculation of the absorption and MCD spectra of metHbF. For more details, we refer the reader to Rots & Zandstra (1982) and Rots (1982).

It is assumed that the metHbF (R state) spectrum from the near-infrared to the near-ultraviolet arises from six 0–0 transitions and four vibronic 0–1 components. The electronic transitions considered are the two lowest allowed  $\pi \rightarrow \pi^*$  ( $a_{1u}$  and  $a_{2u} \rightarrow e_g$  in  $D_{4h}$  notation) and the four lower allowed CT

( $a_{2u}$ ,  $a_{1u}$ ,  $b_{2u}$ , and  $a_{2u}' \rightarrow e_g^d$ ) transitions. All these transitions are of  ${}^6A_{1g} \rightarrow {}^6E_u$  symmetry. Configuration interaction (CI) between these six singly excited states, spin-orbit coupling, and a rhombic distortion result in six electronic transitions, each consisting of a set of six doubly degenerate transitions.

Rather than calculating the  $6 \times 6$  CI matrix, diagonalizing it, and comparing the resulting energies with the positions of the bands in the absorption spectrum, we used a reversed procedure. An absorption-line fit yielded the band energies ( $\epsilon_j$ ), intensities ( $D_j$ ), and widths ( $\Delta_j$ ) of the six 0–0 and the four 0–1 transitions. The band energies of the six 0–0 transitions were then used to determine the energies of the CT transitions before CI,  $\epsilon_i$ , i.e., four of the diagonal elements of the CI matrix and some off-diagonal elements of the  $6 \times 6$  CI matrix. The other matrix elements were taken from an analysis of the hemoglobin monoxide (HbCO) absorption spectrum or were computer calculated. A diagonalization procedure, yielding, per definition, the band energies  $\epsilon_j$ , then provided the configurational functions. From these functions and the band intensities,  $D_j$ , obtained from the fit, the dipole moments of the transitions before CI,  $m_i$ , were then calculated.

Subsequently, spin-orbit coupling and rhombic distortion were taken into account. From the state functions thus obtained, and with some other results from the HbCO analysis, additional computer calculations and some data from the literature, an estimate was made of the dipole strength and MCD of the vibronically induced 0–1 bands,<sup>1</sup> and the temperature-dependent MCD spectra of metHbF were calculated. A calculation of the absorption spectra yielded, as it should, virtually the same spectrum as the experimental one.

According to this calculation, the bands at ~610 nm and that at ~520 nm, each of which has been proposed to be the Q band, i.e., to consist mainly of  $\pi \rightarrow \pi^*$ , both have 48%  $\pi \rightarrow \pi^*$  and 52% CT character. It was shown that the dipole strength of the band at ~485 nm can be accounted for by vibronic coupling.

The spectra of metHbF in the T state and of metHbH<sub>2</sub>O and metHbOH in the R and T states, if one assumes at first that all these derivatives are 100% high spin, are now calculated from the molecular quantities as obtained in the metHbF (R state) analysis by changing only the energies of the four CT transitions in the  $6 \times 6$  CI matrix. The procedure will be described in more detail below.

It is often assumed that the shift in energy of the CT transitions in a series of high-spin ferric heme complexes, with different ligands on the sixth coordination place of the iron, is mainly determined by a change in the energy of the iron  $e_g^d$  orbitals, due to a change in the repulsion of the electro-negative ligand [see, e.g., Nozawa et al. (1980)]. The interpretation (Perutz et al., 1974) for the differences between the absorption spectra of metHbF in the R and in the T state was also based on this assumption.

In our calculation of the spectra of metHbF in the T state and of the high-spin spectra of metHbH<sub>2</sub>O and metHbOH in the R and in the T state, we also make this assumption. All quantities occurring in the heme-F model that are not explicitly affected by a change in energy of the CT transitions are supposed to remain the same.

For the modified energies of the CT transition, we used the following estimate. The energy of the  $e_g^d$  orbital in metHbF ( $\epsilon(e_g^d)$ ) is changed with the amount  $\Delta\epsilon(e_g^d)$  as a parameter to

<sup>1</sup> There are some minor differences in the calculations of the dipole strengths and MCD of the vibronically induced bands between the two aforementioned publications. The results presented here are obtained following the procedure as described in Rots (1982).

yield the modified energy  $\epsilon(e_g^d)$ :

$$\epsilon(e_g^d)' = \epsilon(e_g^d) + \Delta\epsilon(e_g^d) \quad (1)$$

Only the CT transition energies are changed due to  $\Delta\epsilon$  and become

$$E(p \rightarrow e_g^d)' = E(p \rightarrow e_g^d) + \Delta\epsilon(e_g^d) \quad (2)$$

where the  $p$  orbitals are of the  $D_{4h}$  group symmetries  $a_{2u}$ ,  $a_{1u}$ ,  $a_{2u}'$ , and  $b_{2u}$ . Diagonalization gives the modified eigenvalues  $E_j'$  and the configurational coefficients  $(c_i^j)'$ .

The modified transition dipole moments  $m_j'$  are calculated from the  $(c_i^j)'$  and the one-electron transition dipole moments  $m_i$  obtained from metHbF. The Franck-Condon overlap is supposed to be the same as in metHbF.

Rots & Zandstra (1982) and Rots (1982) used in the calculation of the absorption and the temperature-dependent MCD spectra for the bands  $I_a$ ,  $II_b$ ,  $II_a$ , and  $IV_a$  the dipole strengths obtained from the fit of the absorption spectrum,  $D_{J_a}^{\text{fit}}$ , rather than the calculated dipole strengths. In the calculation of the spectra of the modified system, we use for the dipole strengths of these 0-1 bands

$$D_{J_a}' = D_{J_a}^{\text{fit}} + [(D_{J_a}^{\text{calcd}})' - (D_{J_a}^{\text{calcd}})] \quad (3)$$

Thus, we use the "experimental" dipole strengths of metHbF corrected with the difference between the calculated dipole strengths of the modified system and metHbF. The energies of the 0-1 bands are obtained by assuming that the energy difference between a 0-0 band and the corresponding 0-1 band is the same in metHbF and in the modified system:

$$E_{J_a}' = E_j' + (E_{J_a} - E_j) \quad (4)$$

All other quantities required to calculate the MCD and absorption spectra, considering the six doubly degenerate transitions in each  ${}^6A_{1g} \rightarrow {}^6E_u^j$  separately, of the modified system are calculated as by Rots & Zandstra (1982); e.g., the spin-orbit splitting  $(\lambda_j)'$  is calculated from eq 20, with the modified coefficients  $(c_i^j)'$  and the quantities from Table 6. The line-width parameters  $(\Delta_0^j)'$  are obtained from eq 26 with the  $\Delta_j$  from the fit of the absorption spectrum of metHbF.

The parameter  $\Delta\epsilon(e_g^d)$  is determined by trial and error. The best value was chosen by visually comparing the intensity and frequency changes of the low-energy side of band II of the calculated absorption spectrum due to the changes of  $\Delta\epsilon(e_g^d)$  with the experimental changes. In this fashion, minimal variations of about 0.001 eV of  $\Delta\epsilon(e_g^d)$  are clearly distinguishable. For the metHbOH + IHP system, where this method cannot be used,  $\Delta\epsilon(e_g^d)$  was chosen as

$$\Delta\epsilon(e_g^d)_{\text{OH}^+} = \Delta\epsilon(e_g^d)_{\text{OH}^-} + (1/2)(\Delta\epsilon(e_g^d)_F + [\Delta\epsilon(e_g^d)_{\text{H}_2\text{O}^+} - \Delta\epsilon(e_g^d)_{\text{H}_2\text{O}^-}]) \quad (5)$$

where the subscript indicates the ligand on the sixth coordination place of the iron. The superscripts + and - denote the presence and absence of IHP, respectively. Thus, we use for the influence of the  $R \rightarrow T$  transition on the energy of the  $e_g^d$  orbitals in metHbOH the average of the values obtained for metHbH<sub>2</sub>O and metHbF. The values obtained for  $\Delta\epsilon(e_g^d)$  for the various systems are given in Table II,  $\Delta\epsilon(e_g^d)_{\text{OH}^+}$  being calculated by inserting the other values obtained in eq 5.

The experimental metHbF  $\pm$  IHP spectra can directly be compared with the calculated ones. The metHbH<sub>2</sub>O/OH  $\pm$  IHP spectra, however, contain four contributions each, namely, a high-spin and a low-spin contribution of both metHbH<sub>2</sub>O and metHbOH. The way in which the composition of the metHbH<sub>2</sub>O/OH spectra is obtained, as a function of pH and depending on the quaternary structure, is described below.

Table II: Difference between Energy of  $e_g^d$  Orbital in Modified Systems and in metHbF in the R State

derivative	IHP <sup>a</sup>	$\Delta\epsilon(e_g^d)_X^{\pm}/\text{eV}$	$[\Delta\epsilon(e_g^d)_X^+ - \Delta\epsilon(e_g^d)_X^-]/\text{eV}$
metHbF	-	0	
	+	-0.017	-0.017
metHbH <sub>2</sub> O	-	-0.120	
	+	-0.128	-0.008
metHbOH	-	0.020	
	+	0.007	-0.013

<sup>a</sup> The situations + or - correspond to T or R states.

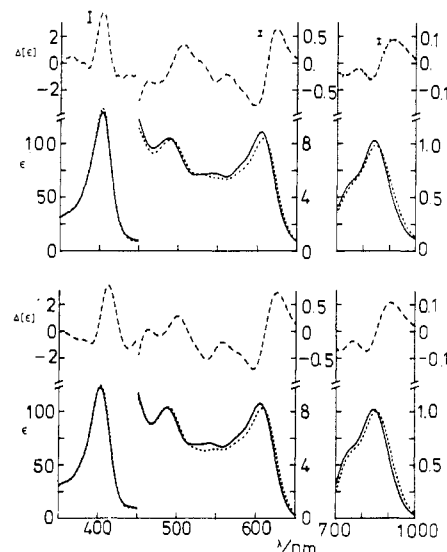


FIGURE 1: Experimental (upper) and calculated (lower) absorption spectra of metHbF in the absence (solid lines) and presence (dotted lines) of IHP and the difference spectra (broken lines).  $\epsilon$  and  $\Delta[\epsilon]$  are expressed in (mM heme  $\text{cm}^{-1}$ ).

Band N, see Figure 5, which occurs at  $\sim 350$  nm in metHbF and overlaps the high-energy side of the Soret band, is not included in the calculation. To facilitate comparison of the calculated and experimental spectra, however, to all calculated high-spin absorption spectra, band N is added, as it was obtained from the fit of the absorption spectrum of metHbF.

## Results

**$R \rightarrow T$  Transition in metHbF.** In Figure 1, the experimental and calculated absorption spectra of metHbF in the absence and presence of IHP are shown. To facilitate comparison, the experimental and calculated difference spectra are also shown. Absorption and MCD difference spectra are defined by

$$\Delta[\epsilon(\nu)] = \epsilon^+(\nu) - \epsilon^-(\nu)$$

$$\Delta\left[\frac{\Delta\epsilon(\nu)}{H}\right] = \frac{\Delta\epsilon^+(\nu)}{H} - \frac{\Delta\epsilon^-(\nu)}{H} \quad (6)$$

The superscripts + and - denote the T (+IHP) and R (-IHP) quaternary structure, respectively. The experimental spectra shown in Figure 1 are obtained in a single experiment. The error bars in the difference spectra indicate the reproducibility. The "calculated" metHbF spectrum in the absence of IHP is the spectrum calculated following Rots & Zandstra (1982), with the six components of each  ${}^6A_{1g} \rightarrow {}^6E_u^j$  transition considered separately. It is essentially determined by the experimental metHbF absorption spectrum. Since the spectrum of T-state metHbF is calculated from the description of the metHbF by only slightly changing one quantity, this spectrum

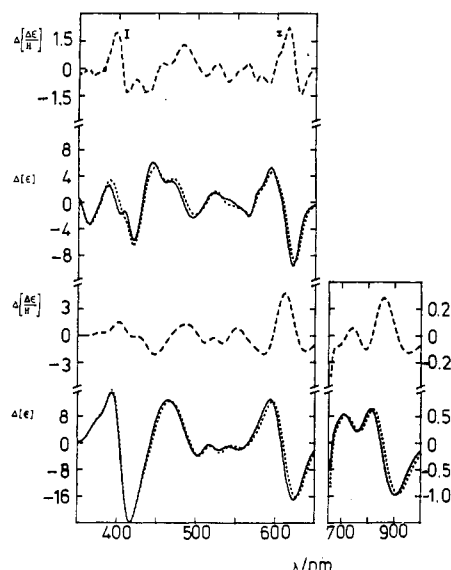


FIGURE 2: Experimental (upper) and calculated (lower) MCD spectra of metHbF in the absence (solid lines) and presence (dotted lines) of IHP and the difference spectra (broken lines).  $\Delta\epsilon/H$  and  $\Delta[\Delta\epsilon/H]$  are expressed in  $(M \text{ heme cm}^{-1})^{-1}$ .

also is mainly determined by the experimental metHbF spectrum. The difference spectrum, however, is almost entirely determined by the heme-F model and the assumptions listed in the preceding section and depends only indirectly, via the model, on the experimental data.

The experimental and calculated MCD spectra of metHbF in the absence and presence of IHP calculated as described in the previous section in the visible and near-UV regions and the calculated spectra in the near-IR, at 7 °C, are shown in Figure 2. The experimental MCD difference spectrum in the visible region is more structured than the calculated one, but the overall features are similar. The calculated MCD difference spectrum in the Soret band is qualitatively correct, but it is much too small. (Since the calculated MCD spectra are about twice as large as the experimental ones, generally the calculated difference spectra should be twice as large as the experimental ones as well.) In most calculations, the model turns out to be rather poor for the Soret-band region. Generally, the calculated MCD spectra are less structured than the experimental ones. Then, the calculated difference spectra are expected to be less structured as well.

**R  $\rightarrow$  T Transition in metHbH<sub>2</sub>O/OH.** Both metHbH<sub>2</sub>O and metHbOH are mixed-spin derivatives, which means that they are partly high-spin  $S = 5/2$ , partly low-spin  $S = 1/2$ . Our hypothesis in this paper is that the effect of the R  $\rightarrow$  T transition on the optical spectra arises from its influence on the energies of the CT transitions. The absorption spectra of low-spin ferric heme compounds are strongly dominated by  $\pi \rightarrow \pi^*$  transitions. Therefore, we assume that an R  $\rightarrow$  T transition does not affect the low-spin ferric heme spectra, and so, the spectral changes upon the R  $\rightarrow$  T transition are supposed to arise entirely from the high-spin contributions to the spectra and possibly from a shift in the high-spin-low-spin equilibrium. Since the relative changes in the experimental Soret-band spectra are very small, which leads to large errors in the difference spectra, and the calculations for the Soret band are not very good, we shall consider mainly the visible region.

metHbH<sub>2</sub>O contains 75% high spin and 25% low spin, both in the R and in the T structure (Perutz et al., 1978; Messana et al., 1970; Gupta et al., 1975). The Soret-band MCD spectra of metHbH<sub>2</sub>O  $\pm$  IHP are dominated by the low-spin contri-

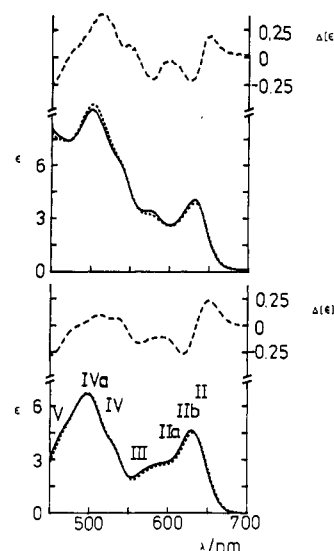


FIGURE 3: Experimental (mixed spin; upper) and calculated high-spin (lower) absorption spectra of metHbH<sub>2</sub>O in the absence (solid lines) and presence (dotted lines) of IHP and the difference spectra (broken lines). The calculated high-spin spectra are multiplied by 0.75 since metHbH<sub>2</sub>O contains 75%  $S = 5/2$ .  $\epsilon$  and  $\Delta[\epsilon]$  are expressed in  $(mM \text{ heme cm}^{-1})^{-1}$ .

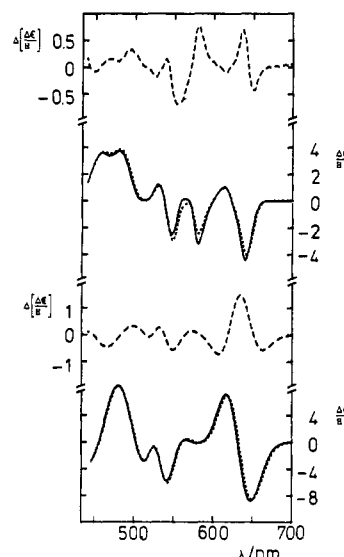


FIGURE 4: Experimental (upper) and calculated high-spin (lower) MCD spectra of metHbH<sub>2</sub>O in the absence (solid lines) and presence (dotted lines) of IHP and the difference spectra (broken lines). The calculated high-spin spectra are multiplied by 0.75.  $\Delta\epsilon/H$  and  $\Delta[\Delta\epsilon/H]$  are expressed in  $(M \text{ heme cm}^{-1})^{-1}$ .

bution. The spectrum of metHbH<sub>2</sub>O in the T state is very much like that of metHbH<sub>2</sub>O in the R state. Upon the R  $\rightarrow$  T transition, the magnitude of the derivative-type band increases slightly. No significant change in frequency occurs. The difference spectrum is of the same magnitude as the Soret-band MCD difference spectrum of metHbF, but the Soret-band MCD spectra of metHbH<sub>2</sub>O  $\pm$  IHP themselves are more than 5 times as large as those of metHbF. This seems to confirm that the R  $\rightarrow$  T transition does not strongly affect the low-spin spectrum.

The experimental absorption and MCD spectra of metHbH<sub>2</sub>O  $\pm$  IHP (pH 5.8) and the difference spectra in the visible region are shown in Figures 3 and 4, respectively. The corresponding calculated high-spin spectra, multiplied by 0.75 according to the high-spin fraction, are also shown in these figures. The positions of the constituting bands are indicated in the calculated absorption spectra in Figure 3. The errors

in the experimental difference spectra in the visible region of metHbH<sub>2</sub>O and of the other metHbH<sub>2</sub>O/OH systems reported in this paper are  $\leq 0.05$  (mM heme cm)<sup>-1</sup> for the absorption and  $\leq 0.1$  (M heme cm T)<sup>-1</sup> for the MCD.

Comparison of the experimental and calculated absorption difference spectra of metHbH<sub>2</sub>O in Figure 3 shows that the calculated spectrum mimics the experimental one fairly well. Only the increase of the dipole strength of band IV<sub>a</sub> upon the R → T transition is substantially stronger in the experimental spectrum than in the calculated one. The difference between the experimental and the calculated absorption spectra should be due to the 25% low-spin contribution. Low-spin ferric heme absorption spectra in the visible region are dominated by two bands in the 580–530-nm region, the Q<sub>00</sub> and Q<sub>01</sub> bands. Band Q<sub>01</sub> usually is stronger than band Q<sub>00</sub>. This is in agreement with the difference between the experimental and the calculated spectra. The Soret band in low-spin ferric heme occurs at lower energy than in high-spin ferric heme. This is the reason why the difference between the experimental and the calculated spectra increases on going from 480 to 450 nm.

The calculated MCD difference spectrum does not match the experimental one very well, but the qualitative features are correct. The low-spin ferric heme MCD spectrum exhibits a negative feature with a minimum at ~580 nm with a rather strong tail to the low-energy side. Therefore, the negative band in the experimental MCD spectra of metHbH<sub>2</sub>O at 580 nm is probably a low-spin contribution. This low-spin contribution also explains why the positive feature at 615 nm is much weaker in the experimental spectrum than in the calculated one. The low-spin ferric heme MCD in the 565–450-nm region is positive and may or may not be very structured, depending on the derivative. Comparison of the calculated high-spin and experimental MCD spectra indicates that in metHbH<sub>2</sub>O, the low-spin contribution in this region is not very structured. The overall difference between the experimental and calculated MCD spectra indicates that the metHbH<sub>2</sub>O low-spin MCD spectrum is rather like the metHbCN one. metHbCN is a 100% low-spin compound. Its MCD spectrum has a positive maximum at ~485 nm. Such a contribution to the metHbH<sub>2</sub>O spectrum would explain why the maximum at 482 nm has increased relative to that at 460 nm, compared with metHbF.

Whereas the high-spin–low-spin equilibrium constant for metHbH<sub>2</sub>O is fairly accurately known, this is not the case for metHbOH. The low-spin fraction  $\alpha$  in metHbOH can be calculated as by Kotani (1968) as

$$\alpha = (\mu_H^2 - \mu^2) / (\mu_H^2 - \mu_L^2) \quad (7)$$

where  $\mu_H$  and  $\mu_L$  are the effective magnetic moments of the high- and low-spin fractions, respectively, and  $\mu$  is the overall effective magnetic moment of metHbOH. The magnetic moment  $\mu$  can be determined from paramagnetic susceptibility experiments. The most serious uncertainty in  $\alpha$  arises from  $\mu$ . Values for  $\mu$  at 293 K have been reported in the range from 3.8 to 4.7  $\mu_B$  (Kotani, 1968; Iizuka & Kotani, 1969; Weissbluth, 1974). Furthermore, it is not clear what value for  $\mu_L$  should be used. The spin-only value is  $3^{1/2} \mu_B$ , but experimentally, magnetic moments have been found for low-spin ferric heme as high as 2.6  $\mu_B$  (Messana et al., 1978), which must be due to a large orbital contribution. For  $\mu_H$ , usually the spin-only value  $\mu_H = 35^{1/2} \mu_B$  is used. The values then obtained for the low-spin fraction  $\alpha$  at 293 K are in the range from 0.40 to ~0.65. Compared with this large uncertainty, lowering the temperature from 293 to 280 K has only a minor influence on  $\alpha$ : it increases by 0.04 (Iizuka & Kotani, 1969). Therefore, we use the same value for  $\alpha$  for the absorption and

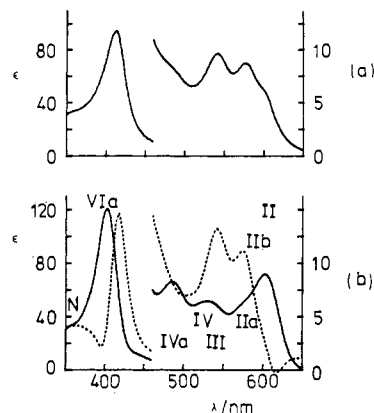


FIGURE 5: (a) Experimental absorption spectrum of metHbOH. (b) Calculated high-spin (solid lines) and low-spin (dotted lines) metHbOH absorption spectra. These spectra are normalized to 100%  $S = 5/2$  and 100%  $S = 1/2$ , respectively. The roman numbers in the calculated spectrum indicate the constituting bands in the high-spin spectrum.  $\epsilon$  is expressed in (mM heme cm)<sup>-1</sup>.

MCD spectra, which were measured at room temperature and at 280 K, respectively.  $\alpha$  is rather arbitrarily chosen as 0.50 ( $\mu_L = 5^{1/2}$ ,  $\mu = 4.47 \mu_B$ ) (Kotani, 1968).

As was mentioned before, at the high pH required to obtain an essentially pure metHbOH sample, IHP can no longer switch the quaternary structure from R to T. From NMR measurements of metHbH<sub>2</sub>O/OH samples in the absence and presence of IHP as a function of pH, Perutz et al. (1978) determined that a change of the quaternary structure from R to T leads to an increase of the paramagnetic susceptibility of metHbOH of 45%. From this, it follows that  $\alpha$  reduces to 0.21 for metHbOH in the T state.

Due to the change in the high-spin–low-spin equilibrium constant upon the R → T transition, the low-spin contribution to the spectra can no longer be ignored. Low-spin metHbOH spectra are obtained from the experimental metHbOH spectra and the calculated high-spin metHbOH spectra as follows:

$$\epsilon_{OH,1/2} = 2(\epsilon_{OH}^{\text{expt}} - 0.5\epsilon_{OH,5/2})$$

$$\frac{\Delta\epsilon}{H_{OH,1/2}} = 2 \left[ \frac{\Delta\epsilon^{\text{expt}}}{H_{OH}} - 0.5 \left( 0.5 \frac{\Delta\epsilon^-}{H_{OH,5/2}} \right) \right] \quad (8)$$

The subscripts OH indicate metHbOH. If a second subscript,  $1/2$  or  $5/2$ , appears, then  $\epsilon$  and  $\Delta\epsilon/H$  indicate the absorbance and MCD of low-spin or high-spin metHbOH, normalized to 100%  $S = 1/2$  or 100%  $S = 5/2$ , respectively. The superscript – denotes the absence of IHP. No superscript appears on the left hand side of eq 8 since the low-spin spectra are supposed to be the same for metHbOH in the R and in the T state. The additional factor 0.5 in the expression for the MCD is a correction factor, which is added because the overall magnitude of the calculated MCD spectra is about twice as large as that of the experimental MCD spectra, as can be seen from the spectra of metHbF and metHbH<sub>2</sub>O. All calculated high-spin MCD spectra shown in the remainder of this paper or used in the calculations are multiplied by 0.5. This is no longer specifically indicated in the figures or the formulas.

Equation 8 introduces another dependence of the calculations on experimental data, but it also provides the means for an extra check: the obtained low-spin spectra should resemble the spectra of low-spin ferric heme compounds. The experimental metHbOH (pH 10.2), the calculated high-spin, and the resulting low-spin metHbOH absorption spectra are shown in Figure 5. In Figure 6, the corresponding MCD spectra are shown. The obtained low-spin metHbOH absorption

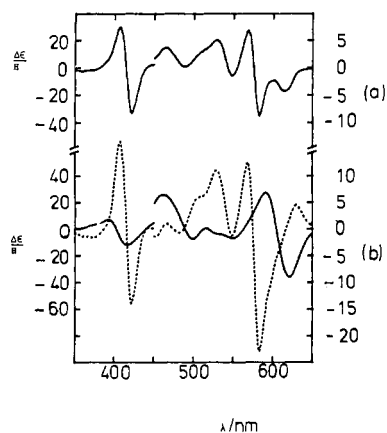


FIGURE 6: (a) Experimental MCD spectrum of metHbOH. (b) Calculated high-spin (solid lines) and low-spin (dotted lines) metHbOH MCD spectra, normalized to 100%  $S = 5/2$  and 100%  $S = 1/2$ , respectively.  $\Delta\epsilon/H$  is expressed in  $(M \text{ heme cm T})^{-1}$ .

spectrum looks very much like a normal low-spin ferric heme absorption spectrum. Only the dips at 615 and 395 nm are unrealistic. The obtained low-spin MCD spectrum is rather like those of metmyoglobin azide and metmyoglobin imidazole, which are 80 and 90% low-spin compounds, respectively (Vickery et al., 1976). The positive feature at 635 nm, however, cannot be correct and is mainly due to the two strong wings of the Gaussian bands used in the calculated spectra. The reasonability of the obtained low-spin spectra implies that the main features of our description of the spectra of metHbOH are likely to be correct.

The proton dissociation of the heme-linked  $H_2O$  molecule in metHb has a  $pK$  of 8.05 (Perutz et al., 1978; Antonini & Brunori, 1971). The proton dissociation can be described by a single equilibrium, despite the fact that four heme groups are involved (Antonini & Brunori, 1971). If one assumes that the equilibrium constant is the same in the R and in the T state (Perutz et al., 1978), the fraction metHbH<sub>2</sub>O in a metHbH<sub>2</sub>O/OH sample at a given pH, indicated by  $\beta$ , is given by

$$\beta = (1 + 10^{pH-8.05})^{-1} \quad (9)$$

Then the composition of an absorption spectrum of metHbH<sub>2</sub>O/OH in the absence or presence of IHP is given by

$$\epsilon_{H_2O/OH}^+ = \beta(0.75\epsilon_{H_2O,5/2}^+ + 0.25\epsilon_{H_2O,1/2}^+) + (1 - \beta)[(1 - \alpha^+)\epsilon_{OH,5/2}^+ + \alpha^+\epsilon_{OH,1/2}^+] \quad (10)$$

where  $\alpha^+ = 0.21$  and  $\alpha^- = 0.50$ . The difference spectrum becomes

$$\Delta[\epsilon] = \epsilon_{H_2O/OH}^+ - \epsilon_{H_2O/OH}^- = 0.75\beta(\epsilon_{H_2O,5/2}^+ - \epsilon_{H_2O,5/2}^-) + (1 - \beta)(0.79\epsilon_{OH,5/2}^+ - 0.50\epsilon_{OH,5/2}^- - 0.29\epsilon_{OH,1/2}^-) \quad (11)$$

The expressions for the MCD are completely analogous to eq 10 and 11. Experimental difference spectra can only be obtained for  $pH \lesssim 7.5$ , which corresponds to  $\beta \gtrsim 0.8$ . The experimental and calculated difference absorption spectra for a series of pH values  $5.7 < pH < 7.5$  and the calculated absorption difference spectrum for pure metHbOH are shown in Figure 7. The corresponding difference MCD spectra are shown in Figure 8. To facilitate comparison, vertical lines are drawn through the maxima in the absorption difference spectra at 608 nm in the pH 7.45 spectra and at 512 nm in the pH 5.8 spectra. All the overall changes in the calculated and experimental difference spectra as a function of pH are similar: on going to higher pH, the derivative-type feature

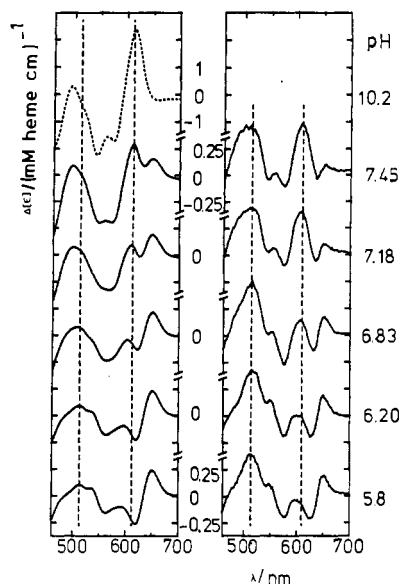


FIGURE 7: Calculated (left) and experimental (right) absorption difference spectra of metHbH<sub>2</sub>O/OH at various pH values.

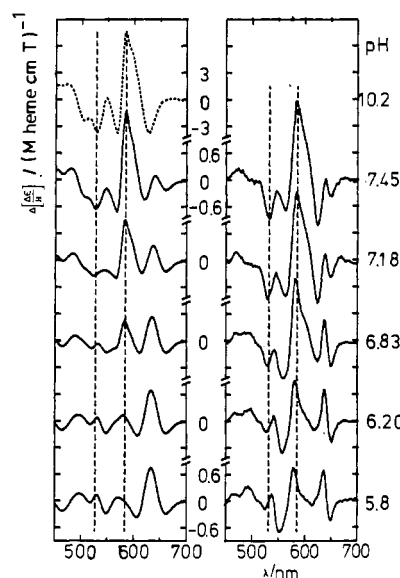


FIGURE 8: Calculated (left) and experimental (right) MCD difference spectra of metHbH<sub>2</sub>O/OH at various pH values.

at 640 nm weakens; the maximum at 595 nm grows strongly and is shifted to the red. The shoulder at 540 nm goes to lower  $\Delta[\epsilon]$  values, such that at high pH it becomes a minimum, and the shoulder on the blue side of the 512-nm line grows, turning into a maximum at high pH. The most serious disagreement between the experimental and calculated difference spectra can most easily be described by saying that the calculated spectra seem to have a bent base line: at higher energy, the overall calculated difference spectra are positioned at too low  $\Delta[\epsilon]$  values. This effect is worst at the high pH values. More will be said about this in the next section. In the spectra in Figure 8, vertical lines are drawn through the maxima at 585 nm and the minima at  $\sim 530$  nm in the pH 7.45 MCD difference spectra, to facilitate comparison. In these spectra also, the overall changes in the calculated and experimental difference spectra as a function of pH are similar, toward higher pH, and the minimum and maximum at  $\sim 650$  and  $635$  nm, respectively, weaken: they have disappeared in the calculated metHbOH MCD difference spectrum. The minimum at 615 nm and the maximum at  $\sim 575$  nm shift to the red. This maximum grows very strongly. The 525-nm minimum shifts

also to the red and becomes more intense. The high-energy region is not very clear, but the 495-nm maximum seems to weaken whereas a new maximum grows at slightly higher energy, toward higher pH. The most serious difference between the calculated and experimental spectra arises from the maximum and minimum in the metHbH<sub>2</sub>O spectrum at ~575 and 550 nm, respectively, which are too weak in the calculated spectrum. This is the main reason why the 575–585-nm maximum seems to grow more quickly in the experimental spectra toward higher pH than in the calculated spectra.

### Discussion

If one considers the limitations of the heme-F model, described by Rots & Zandstra (1982), the agreement between the experimental and calculated metHbF difference spectra seems to justify the conclusion that in this derivative, the changes occurring in the absorption and MCD spectra upon a change in quaternary structure from R to T arise mainly from a lowering of the energy of the  $e_g^d$  orbitals.

A fairly reasonable description of the metHbH<sub>2</sub>O spectra is obtained from the heme-F model by changing only the energy of the  $e_g^d$  orbitals (and taking into account that the high-spin fraction reduces from 1 to 0.75). The influence of replacing the F<sup>−</sup> ligand by H<sub>2</sub>O on the spectra is much larger than that of the quaternary structure change metHbF(R) → metHbF(T). Provided that the replacement of the ligand and the quaternary structure change affect the heme in a similar way, i.e., that the R → T transition only has an influence on the heme through the fifth (proximal histidine) or the sixth (F<sup>−</sup>) coordination place on the iron, the reasonability of the obtained metHbH<sub>2</sub>O spectra also indicates that for the much smaller effect of the quaternary structure change metHbF(R) → metHbF(T), it may be a fairly good approximation to assume that all intrinsic heme properties that affect the optical spectra, apart from the energy of the  $e_g^d$  orbitals, remain unaltered.

In the calculation of the influence of the R → T transition on the absorption spectrum of metHbH<sub>2</sub>O, the increase of the dipole strength of band IV<sub>a</sub> is too small. This may be due to the major approximations made in the calculation of the dipole strengths of vibronically induced bands (Rots & Zandstra, 1982). The possibility cannot be ruled out, however, that changes do occur in the porphyrin part of the heme, upon the R → T transition, which result in a stronger vibronic coupling. Some small changes in porphyrin vibrations due to the quaternary structure change have been found in resonance Raman experiments (Shelnutt et al., 1979; Shelnutt, 1980). The largest disagreement between the calculated and experimental MCD difference spectra of metHbH<sub>2</sub>O occurs at approximately the position of the low-spin band at 580 nm. A reason for this may be that the assumption that a low-spin spectrum does not change upon an R → T transition is incorrect, at least for the MCD. However, it may also be caused by the overlap between bands II<sub>a</sub> and III, which is too large in the MCD calculations, resulting in a smaller feature in the calculated MCD difference spectrum.

The values for  $\Delta[\epsilon]$  in the calculated metHbH<sub>2</sub>O/OH absorption difference spectra in the higher energy region are too low, especially in the spectra for higher pH. One explanation for this would be that the decrease of the low-spin fraction  $\alpha$  of metHbOH upon the R → T transition, used in the calculation, is too large. If a lower value was used for the magnetic moment  $\mu$  of metHbOH in eq 7, then also a smaller decrease of  $\alpha$  would have resulted. However, a smaller decrease of the low-spin fraction would also lead to smaller maxima in the absorption difference spectra at 608 nm and

in the MCD difference spectra at 585 nm, which is undesirable. A more likely explanation seems to be that the calculated dipole strength of the high-spin band IV<sub>a</sub> is too small. If the dipole strength of this band were larger, then the low-spin absorption spectrum obtained would have had lower extinction coefficients in the 500–460-nm region, which would have resulted in higher values of  $\Delta[\epsilon]$  in this region of the calculated absorption difference spectra. Another source of possible error in the metHbH<sub>2</sub>O/OH calculation is the assumption that the proton dissociation of the heme-linked water molecule can be described as a single equilibrium with a pK that is unchanged by an R → T transition. This is probably an oversimplification (Gupta & Mildvan, 1975), but a more reliable description of the proton dissociation as a function of pH, in the absence and presence of IHP, is not yet known.

Although certain differences occur between the calculated absorption and MCD difference spectra of metHbF and metHbH<sub>2</sub>O/OH and the corresponding experimental ones, the calculated spectra generally match the experimental ones reasonably well. Therefore, it seems likely that the differences in the absorption and MCD spectra upon an R → T transition are mainly due to a lowering of the energy of the  $e_g^d$  orbitals and, in the case of metHbH<sub>2</sub>O/OH, to an increase of the high-spin fraction of the metHbOH component.

As will be argued elsewhere, this reduction in the energy of the iron  $e_g^d$  orbitals in metHbF upon the R → T transition is most likely due to a lengthening of the Fe–N<sub>1</sub> (proximal histidine) bond length or to a change in the position of the proximal histidine resulting in a reduced interaction between the imidazole and the iron. It is unlikely that the position of the iron changes significantly with respect to the porphyrin plane. Such an assignment need not be in conflict with the results of resonance Raman experiments as reported by Asher et al. (1981) and is in agreement with the changes occurring in the absorption and MCD spectra of metHbF upon a change in pH. In metHbH<sub>2</sub>O and metHbOH, however, the possibility of a significant change in the position of the iron relative to the porphyrin plane upon a quaternary structure change cannot be ruled out.

### Acknowledgments

We thank H. J. Panneman for his assistance with some of the experiments.

### References

- Antonini, E., & Brunori, M. (1971) *Hemoglobin and Myoglobin in Their Reactions with Ligands*, North-Holland, Amsterdam.
- Asher, S. A., Adams, M. L., & Shuster, T. M. (1981) *Biochemistry* 20, 3339.
- Eaton, W. A., & Hochstrasser, R. M. (1968) *J. Chem. Phys.* 49, 985.
- Fermi, G., & Perutz, M. F. (1977) *J. Mol. Biol.* 114, 421.
- Gupta, R. K., & Mildvan, A. S. (1975) *J. Biol. Chem.* 250, 246.
- Iizuka, T., & Kotani, M. (1969) *Biochim. Biophys. Acta* 194, 351.
- Kotani, M. (1968) *Adv. Quantum Chem.* 4, 227.
- Linder, R. E., Records, R., Bart, G., Bunnenberg, E., Djerassi, C., Hedlund, B. E., Rosenberg, A., Seamans, L., & Moscowitz, A. (1980) *Biophys. Chem.* 12, 143.
- Messana, C., Cerdonio, M., Shenkin, P., Noble, R. W., Fermi, G., Perutz, R. N., & Perutz, M. F. (1978) *Biochemistry* 17, 3652.
- Nozawa, T., Ookubo, S., & Hatano, M. (1980) *J. Inorg. Biochem.* 12, 253.



- Perutz, M. F. (1979) *Annu. Rev. Biochem.* 48, 327.  
 Perutz, M. F., Fersht, A. R., Simon, S. R., & Roberts, G. C. K. (1974a) *Biochemistry* 13, 2174.  
 Perutz, M. F., Heidner, E. J., Ladner, J. E., Beetlestone, J. G., Ho, C., & Slade, E. F. (1974b) *Biochemistry* 13, 2187.  
 Perutz, M. F., Sanders, J. K. M., Chenergy, D. H., Noble, R. W., Pennelly, R. R., Fung, L. W.-M., Ho, C., Giannini, I., Pörschke, D., & Winkler, H. (1978) *Biochemistry* 17, 3640.  
 Rots, M. J. F. (1982) Ph.D. Thesis, University of Groningen.  
 Rots, M. J. F., & Zandstra, P. J. (1982) *Mol. Phys.* 46, 1283.  
 Shelnutt, J. A. (1980) *International Conference on Raman Spectroscopy*, 7th, Ottawa, Aug 1980, Elsevier/North-Holland, New York.  
 Shelnutt, J. A., Rousseau, D. L., Friedman, J. M., & Simon, S. R. (1979) *Proc. Natl. Acad. Sci. U.S.A.* 76, 4409.  
 Smith, D. W., & Williams, R. J. P. (1970) *Struct. Bonding (Berlin)* 7, 1.  
 Vickery, L., Nozawa, T., & Sauer, K. (1976) *J. Am. Chem. Soc.* 98, 343.  
 Weissbluth, M. (1974) *Hemoglobin, Cooperativity and Electronic Properties*, Springer-Verlag, Berlin.  
 Zerner, M., Gouterman, M., & Kobayashi, H. (1966) *Theor. Chim. Acta* 6, 363.

## Proton NMR Spectroscopy of Cytochrome *c*-554 from *Alcaligenes faecalis*<sup>†</sup>

Russell Timkovich\* and Margaret S. Cork

**ABSTRACT:** Cytochrome *c*-554 from the bacterium *Alcaligenes faecalis* (ATCC 8750) is a respiratory electron-transport protein homologous to other members of the cytochrome *c* family. Its structure has been studied by <sup>1</sup>H NMR spectroscopy in both the ferric and ferrous states. The ferric spectrum is characterized by downfield hyperfine-shifted heme methyl resonances at 46.25, 43.60, 38.40, and 36.73 ppm (25 °C, pH 7.1). Chemical shifts of these resonances change with temperature opposite to expectations derived from Curie's law. The pH behavior of the hyperfine-shifted resonances titrates

with a pK of 6.3 that has been interpreted as due to ionization of a heme propionate. In the ferrous state, heme methyl, meso, and thioether bridge resonances have been observed and assigned. All aromatic protons have been assigned according to the side chain of origin, and the structural environment about the sole tryptophan residue has been examined. The electron-transfer rate between ferric and ferrous forms has been estimated to be on the order of  $3 \times 10^8 \text{ M}^{-1} \text{ s}^{-1}$ , which is the largest such self-exchange rate yet observed for a cytochrome.

**C**omparison of cytochrome structures and properties contributes to understanding the function of these ubiquitous electron-transport proteins. Cytochromes *c* play such an integral role in respiration that they are found widely distributed not only in eukaryotic cells but also in almost all prokaryotic cells. Proton NMR spectroscopy is a useful technique for making structural comparisons among cytochromes *c*. It is made more powerful by the three-dimensional data available from X-ray crystallography on a limited number of archetype cytochromes and the growing number of NMR assignments that have been achieved.

Recently the isolation and partial characterization of a low molecular weight cytochrome *c* were reported for the bacterium *Alcaligenes faecalis* (ATCC 8750) (Timkovich et al., 1982). On the basis of its visible spectrum in the reduced state, it has been termed cytochrome *c*-554. It functions in the electron-transport chain of *Alcaligenes*, donating electrons to a soluble nitrite reductase during denitrification and presumably to a membrane cytochrome oxidase during aerobic respiration. It has approximately 86 amino acids, and its amino acid composition is similar to that of cytochrome *c*-551 from *Pseudomonas aeruginosa*. Cytochromes with this relatively

low molecular weight appear to constitute a subclassification of the general cytochrome *c* family (Dickerson et al., 1976). *Pseudomonas* cytochrome *c*-551 has been studied by X-ray crystallography (Almasy & Dickerson, 1978) and by proton NMR (Keller, R. M., et al., 1976; Moore et al., 1977; Chao et al., 1979). Potentially homologous photosynthetic cytochromes *c*-553 from cyanobacteria have also recently been the subject of an NMR investigation (Ulrich et al., 1982). Structural results have revealed interesting differences between these low molecular weight cytochromes and the larger eukaryotic cytochrome *c* that include different chirality about the axial sulfur ligand (Senn et al., 1980) and a different distribution of spin density in the oxidized form (Keller & Wuthrich, 1978a,b). It is plausible that further differences in the precise structure exist among the many variants of cytochrome.

Proton NMR data are presented here for cytochrome *c*-554 from *Alcaligenes*. The results broaden the basis for comparisons of cytochrome structure and contribute assignment data for critical elements of the protein. Features of the *c*-554 spectra are unique and have not been previously observed for a member of the cytochrome *c* family.

### Materials and Methods

*Alcaligenes faecalis* (ATCC 8750) was cultured and the cytochrome *c*-554 purified as described previously (Timkovich et al., 1982). The spectroscopic purity ratio of the absorbance at 409 nm to that at 280 nm was greater than 5.2 for all

<sup>†</sup> From the Department of Chemistry, Illinois Institute of Technology, Chicago, Illinois 60616. Received April 8, 1983. Financial support was provided by Grant GM-23869 from the National Institutes of Health. The NMR facility was supported by a grant from the NIGMS Shared Instrumentation Program of the National Institutes of Health (GM-26071-02S1).